Pure Appl. Chem., Vol. 81, No. 8, pp. 1489–1498, 2009.
doi:10.1351/PAC-CON-08-08-20

Nanostructured oxides for energy storage applications in batteries and supercapacitors*

Amreesh Chandra, Alexander J. Roberts, Eric Lam How Yee, and Robert C. T. Slade‡

Chemical Sciences, University of Surrey, Guildford GU2 7XH, UK

Abstract: Nanostructured materials are extensively investigated for application in energy storage and power generation devices. This paper deals with the synthesis and characterization of nanomaterials based on oxides of vanadium and with their application as electrode materials for energy storage systems viz. supercapacitors. These nano-oxides have been synthesized using a hydrothermal route in the presence of templates: 1-hexadecylamine, Tweens and Brij types. Using templates during synthesis enables tailoring of the particle morphology and physical characteristics of synthesized powders. Broad X-ray diffraction peaks show the formation of nanoparticles, confirmed using scanning electron microscopy (SEM) and transmission electron microscopy (TEM) investigations. SEM studies show that a large range of nanostructures such as needles, fibers, particles, etc. can be synthesized. These particles have varying surface areas and electrical conductivity. Enhancement of surface area as much as seven times relative to surface areas of starting parent materials has been observed. These properties make such materials ideal candidates for application as electrode materials in supercapacitors. Assembly and characterization of supercapacitors based on electrodes containing these active nano-oxides are discussed. Specific capacitance of >100 F g^{-1} has been observed. The specific capacitance decreases with cycling: causes of this phenomenon are presented.

Keywords: supercapacitors; nanomaterials; electron microscopy; particle synthesis, electrodes.

INTRODUCTION

The last few decades have witnessed a tremendous growth in the search for alternative energy systems. This research area is now a worldwide focus due to the realization of the threat of global warming and acceptance of the fact that resources of conventional energy sources such as fossil hydrocarbon fuel, coal, etc. are limited. Some major research in this area focuses on wind and solar energy, fuel cells, microbial fuel cells, piezoelectric energy harvesters, and supercapacitors [1–9]. It is suggested that the next few decades will be based on fulfilling the energy needs by carefully balancing traditional energy sources with renewable energy resources [1]. As of today, major limiting factors for large-scale application of renewable sources are: (a) fluctuation independent of demand, (b) high cost, and (c) need for alternative storage methods/techniques, etc. [1]. Amongst the alternative energy storage systems, supercapacitors have attracted widespread interest [8,10].

*Paper based on a presentation at the 8th Conference on Solid State Chemistry, 6–11 July 2008, Bratislava, Slovakia. Other presentations are published in this issue, pp. 1345–1534.

‡Corresponding author

Supercapacitors are compact electrochemical capacitors that can store a high amount of energy which can then be discharged at rates demanded by different specific applications [8]. Supercapacitors are finding application in consumer electronics, hybrid electric vehicles, industrial power management, defense industry, communication, etc. [11–16]. Energy in supercapacitors is stored in two possible ways: electrochemical double-layer capacitance (EDLC) and Faradaic pseudo-capacitance, which involves redox processes [8]. Depending upon the electrodes used, a supercapacitor can be broadly classified as an EDLC, a pseudo-capacitor, or a hybrid capacitor [8]. The power and energy densities of these devices strongly depend upon the performance of the electrode materials. Desired parameters for efficient electrode materials are high conductivity, tailorable morphology, large surface area with controlled pore structure, low cost, high aspect ratio, thermal stability, and reproducibility. Nanomaterials have been shown to possess most of the above-mentioned characteristics and therefore are being extensively investigated as electrode materials in energy systems. In operation, these nanomaterials can function both via nonspecific adsorption and via intercalation–deintercalation. Supercapacitors marketed today are mostly based on RuO_2 or carbon. RuO_2 is very expensive and toxic, whereas carbon electrode-based supercapacitors have limited energy storage capacity. Therefore, other metal oxides based on manganese [17,18], vanadium [7], molybdenum [19], lithium [20,21], tin [22], etc. are being investigated as alternatives to RuO_2. This paper reports the synthesis and characterization of nano-oxides based on vanadium and their application in supercapacitors. The typical behavior of such supercapacitors is also presented.

EXPERIMENTAL

Vanadium oxide-based nanopowders were synthesized via a hydrothermal route in the presence of different templates, namely, 1-hexadecylamine, Tween, and the Brij families of templates. The representative structures of these three templates are shown in Figs. 1a, b, and c. The details of synthesis are reported elsewhere [7].

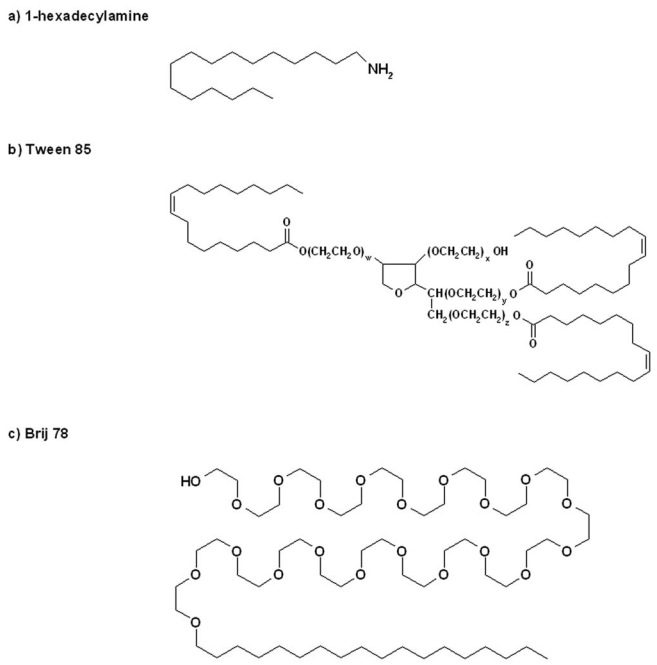

Fig. 1 Structure of the three templates used: (a) 1-hexadecylamine, (b) Tween 85, and (c) Brij 78.

X-ray diffraction (XRD) powder profiles were recorded on a PANalytical X'Pert Pro PW PW3719 diffractometer using CuK_α radiation and an X'Celerator detector. SEM micrographs were recorded using a Hitachi S-3200N instrument. TEM micrographs were recorded using a Philips/FEI CM200. Samples for nitrogen sorption analysis were first outgassed at 200 °C for 12 h using a Micromeritics Flowprep 060 before transferring to a Micromeritics Gemini V Surface Area and Pore Size Analyser. Impedance measurements were carried out using a Solartron 1260 impedance analyzer in the frequency range 1 Hz–100 kHz (oscillating voltage 0.5 V).

Composite films for use as electrodes were prepared by the doctor blade method using a Sheen 1133N automatic film applicator. The active material (synthesized VO_2 powders) was mixed with polymer (PVdF) and graphite in the weight ratio 60:30:10. The mixed powders were thoroughly stirred in acetone at 80 °C until a slurry of optimum viscosity was obtained. The slurry was then poured onto a glass top. Composite films of thickness ~100 μm were obtained by running the blade over the slurry. The films were left to dry on the glass top before being lifted. 13-mm discs were cut and assembled to a constant torque of 2 N m^{-1} in test cells across a glass fiber separator presoaked in $(NH_4)_2SO_4$ (aq., 2 mol dm^{-3}) electrolyte. Symmetrical supercapacitors were assembled using the design reported by White and Slade [23]. Figure 2 shows the schematic of basic supercapacitor (Fig. 2a) and the fabricated supercapacitor cells (Fig. 2b,c).

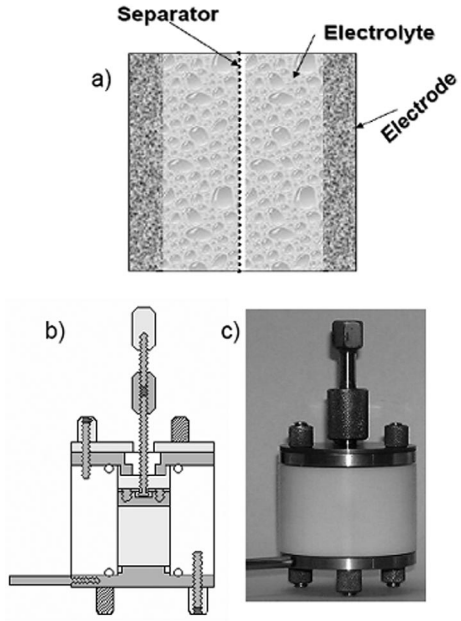

Fig. 2 Schematic of (a) a basic supercapacitor (b) engineering drawing for a supercapacitor cell, and (c) a fabricated supercapacitor cell.

Galvanostatic cycling of the assembled test cells was carried out using a Solatron 1480 multistat, with a 1255B Frequency Response Analyzer. Supercapacitor cells were cycled 200 times between 0 and 1 V at currents of ±1 mA cm^{-2} before being allowed to self-discharge under open circuit conditions.

RESULTS AND DISCUSSIONS

Figures 3a, b, and c show the XRD patterns of VO_2 materials synthesized in the presence of three different templates. No evidence of the presence of unreacted started components was observed. The strik-

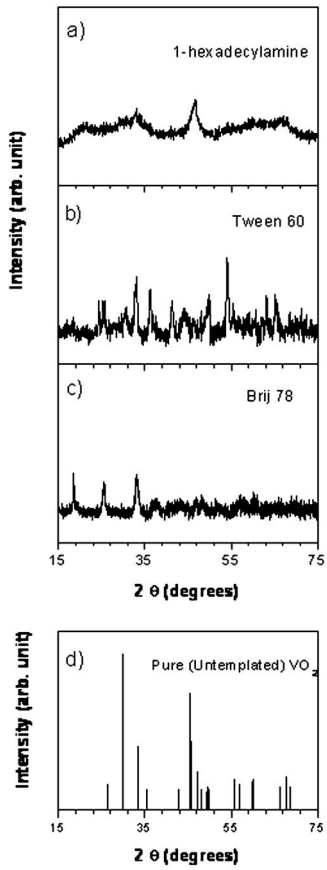

Fig. 3 XRD patterns of VO_2 powders synthesized in the presence of (a) 1-hexadecylamine, (b) Tween, and (c) Brij templates.

ing feature is the significant modification in the diffraction profiles in comparison to the diffraction pattern of pure VO_2, which is shown in Fig. 3d. The broad diffraction peaks clearly suggest either of two possibilities, namely, (i) formation of nanoparticles or (ii) appearance of an amorphous phase. Although the peaks do appear broad in all the synthesized powders, they are indexable by considering VO_2 as the major phase. It should also be mentioned that coexistence of some other oxide phases of V such as V_2O_3 and V_3O_7 was also observed in some cases. The phase fractions of other oxides were minimal and so the overall physical property variations of the samples (due to these impurity phases) are not expected to be significant. XRD studies do point toward the modification of particle morphology/size of synthesized VO_2 particles, but such claims cannot be made based on the XRD data alone. It becomes imperative to carry out microscopic investigations to further understand the modification in particle morphology and size.

SEM micrographs shown in Figs. 4a, b, and c depict the various morphologies which can be obtained in VO_2 particles synthesized in the presence of three different templates. The details of these investigations are as follows:

- The VO_2 nanoparticles synthesized in the presence of 1-hexadecylamine show layered morphology (Fig. 4a).

- In the second case, when Brij templates are used, nanofibrous morphology is observed (Fig. 4b). These nanofibers seem quite evenly distributed within the sample and, in some cases, are as long as 50 μm.
- In the third case, when Tween templates are used, a more "flaky" morphology is observed (see Fig. 4c).

As the synthesis steps were otherwise kept similar, the appearance of different morphologies is believed to be a direct consequence of the differing structures of the templates. Different templates affect the final particle structure in a different manner, and their subsequent removal during synthesis will force different macroscopic morphologies.

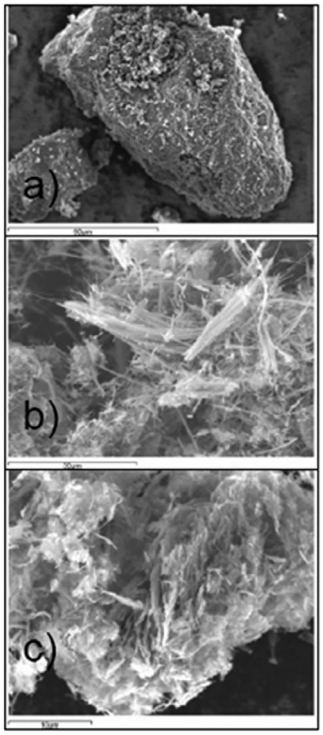

Fig. 4 SEM micrographs for VO_2 powders synthesized in the presence of (a) 1-hexadecylamine, (b) Brij, and (c) Tween templates. The scale bar in (a) and (c) corresponds to 10 μm while for (b) it corresponds to 30 μm.

Figures 5a and b depict the representative TEM micrographs of the various templated-VO_2 samples. It is observed that the microscopic morphologies of the synthesized VO_2 powders are seemingly nanofibrous. The major difference is the extent to which these nanofibers align and/or their varying dimensions. Samples synthesized in the presence of Brij templates are more aligned and longer nanofibers. It must be mentioned that the Brij template molecule is much larger and lower dimensional in comparison to the 1-hexadcylamine template (see Fig. 1). Both SEM and TEM studies clearly suggest that the synthesized powders can be expected to have varying surface area and pore structures in comparison to that of starting parent V_2O_5 powders.

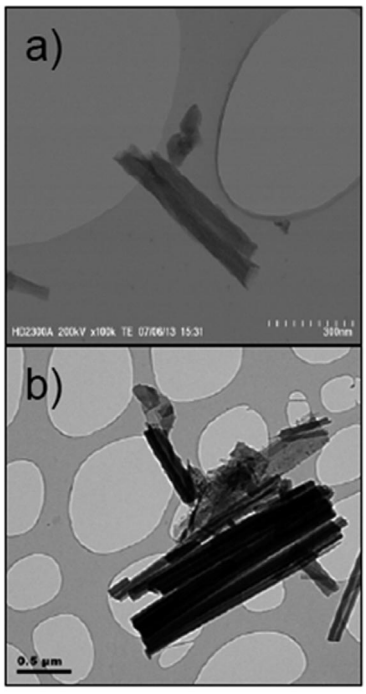

Fig. 5 Representative TEM micrographs of VO_2 powders synthesized in the presence of (a) 1-hexadecylamine and (b) Brij 78 template. The scale bar in (a) corresponds to 0.3 µm while in (b) it corresponds to 0.5 µm.

Nitrogen soprtion analysis at 77 K of all materials revealed both type I and IV behavior [7]. The isotherm at low pressures shows rapid uptake of nitrogen, but no plateau was observed in the nitrogen uptake nor upon desorption. This clearly suggests the presence of both meso- and micropores [7,24,25]. The hysteresis loops could be classified as a combination of H3 and H4, suggesting slit-shaped pores formed through the aggregation of platy particles [7,24,25]. The maximum specific surface area calculated using the BET model was ~70 $m^2\ g^{-1}$; surface areas of the tailored particles are increasing by 6–7 times as compared to the surface area of the starting V_2O_5 powders, which had a surface area ~10 $m^2\ g^{-1}$. Further, it was observed that the variation in surface area not only depends upon the template that is used during synthesis but also on the original template:parent oxide mass ratio used in the synthesis. This is shown in Fig. 6. From this figure, it is clear that the use of different sized templates results in modification of the surface area to a different extent. The maximum enhancement is observed when the template to parent (V_2O_5) powder mass ratio is 1:1. With higher amounts of templates the observed values of surface area decrease. This can be expected as higher concentration of templates will result in template agglomeration which in turn will hamper the optimum growth of particles with highest surface area. Similar behavior has been observed when the particles were synthesized in the presence of different Brij templates. As the investigations above suggest, the available pore structures in these materials will also be different. This is confirmed in Fig. 7, which depicts the variation in pore volume as a function of pore diameter in VO_2 powders synthesized in the presence of differing Tween templates. In particles synthesized in the presence of three differing templates, a modal pore diameter in the range 40–60 Å was observed, whereas the observed pore volumes were in the range of 0.02–0.18 $cm^3\ g^{-1}$.

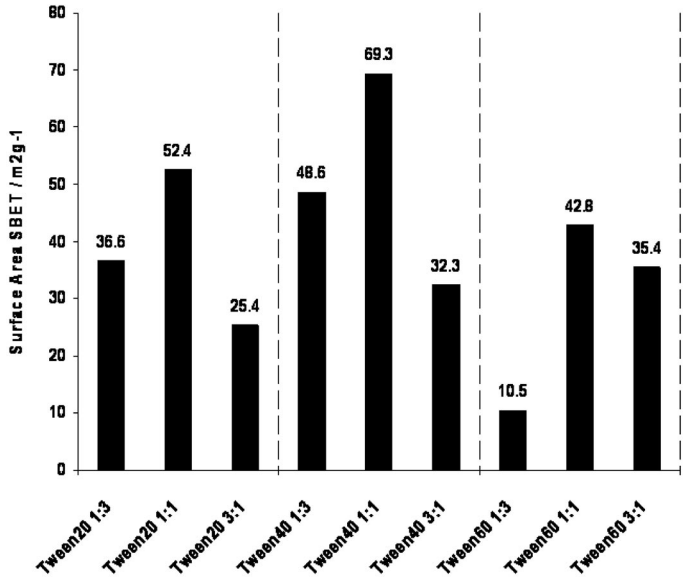

Fig. 6 Variation of surface area for synthesized VO_2 as a function of Tween templates and their template: parent oxide mass ratio.

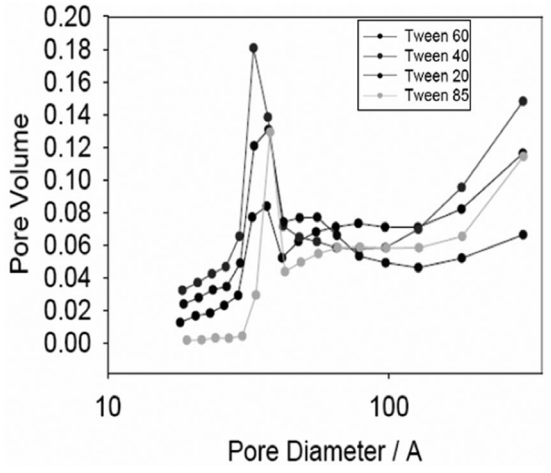

Fig. 7 Variation of pore volume vs. pore diameter observed in VO_2 powders synthesized in the presence of different Tween templates.

Morphology and surface area studies discussed above clearly suggest that VO_2 powders synthesized in the presence of different templates will also show differing electrical conductivity. Figure 8 shows the variation of conductivity in various templated products at room temperature. Conductivity enhancement of ~3–5 orders of magnitude (as compared to conductivity of parent powder) was observed. This is expected to be a direct consequence of the formation of nanosized systems with large surface area and different pore structures, to provide new pathways for the storage and motion of ionic charge carriers. This increase in conductivity, surface area, and tailored pore structure makes these synthesized powders ideal candidates for charge (ionic) storage and/or also as medium electronic conductivity materials. Such materials have been used as electrode materials in energy storage system, namely, "supercapacitors", and may also be applicable in batteries.

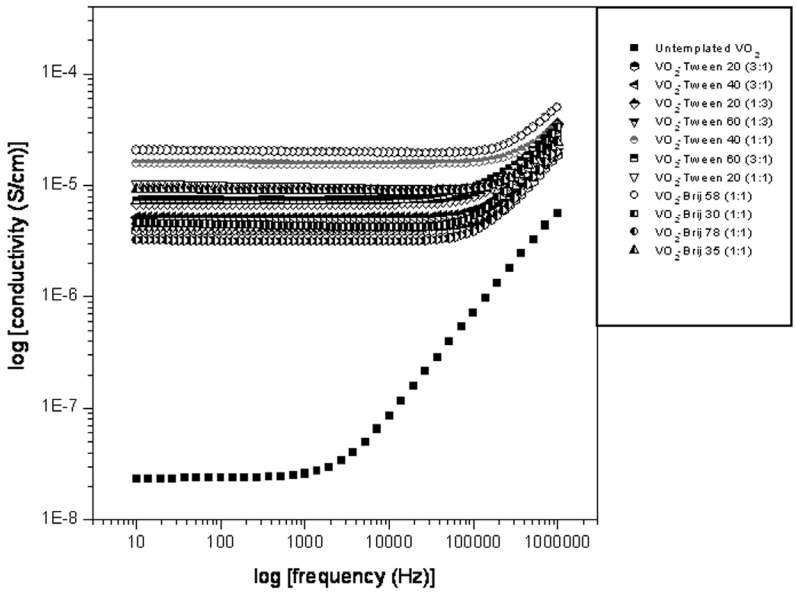

Fig. 8 Variation of electrical conductivity as a function of frequency in VO_2 powders synthesized in the presence of different templates.

Circular electrodes of 13 mm diameter were cut from films obtained using the doctor blade method (see Experimental section). SEM was carried out on both sides of the film to confirm uniform particle dispersion on the film surfaces. Assembly of symmetrical supercapacitors and design details have been reported earlier [23] and in the Experimental section above. The specific capacitance values were evaluated using the relation $C = i(\Delta t)/m(\Delta V)$, where i is the current, m is the mass of active material used in both the electrodes, Δt is time required to change the potential difference (V) by ΔV. In the present case, the supercapacitors were charged within the limits ±1 V.

A typical charge–discharge curve is shown in Fig. 9. The discharge characteristics have been found to be almost linear, confirming capacitative behavior of the supercapacitor. The initial abrupt change during charging and discharging is due to the ohmic loss across the internal resistance of the cells. The capacitances observed when different templated VO_2 materials were used are in the range >100 F g^{-1} or more. The specific capacitance decreases after prolonged cycling. This decrease can be attributed to charge loss resulting from irreversible reactions which can occur at the electrode–electrolyte interface. This may result in formation of certain insulating regions along the surface of the electrode, thereby decreasing the ability of the electrodes to store charge. This is similar to the factors which result in performance losses in fuel cells [3]. More detailed investigation is currently in progress to understand this phenomenon. As VO_2 materials are cheaper and less toxic compared to RuO_2, these can economically act as alternative to RuO_2 in electrodes for alternative energy systems.

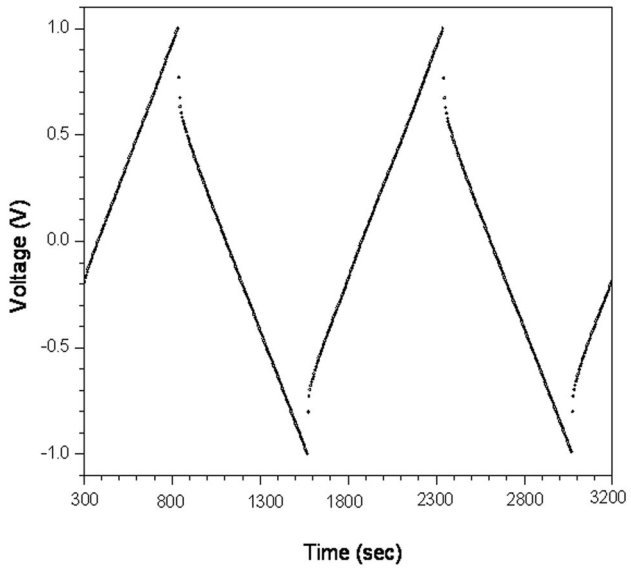

Fig. 9 Typical charge–discharge curve for a symmetrical supercapacitor assembled using VO_2-containing electrode films. The VO_2 powder used in the depicted example was synthesized in the presence of Brij 35 template.

CONCLUSIONS

Synthesis of nanostructured VO_2 in the presence of three different templates is reported. SEM investigation shows formation of particles with differing morphologies: layered, flaky, or fibrous. TEM studies have shown that the microscopic morphology of synthesized powders is nanofibrous. The dimensions of these nanofibrous particles strongly depend on the templates used during synthesis. Large modifications of particle surface area, pore volume, and pore diameter are observed. The increase in surface area is found to depend not only upon the template that is used but also on the mass ratio of template and parent oxide used during synthesis. Enhancement by ~3–5 orders of magnitude in electrical conductivity (in comparison to electrical conductivity of starting powder) is observed. Tailorable surface area, pore structure, and electrical conductivity make these powders ideal candidates for application as electrode materials in energy storage systems such as supercapacitors and batteries. Assembly and characterization of supercapacitors are reported. These studies show that templated VO_2 material may act as a cheap and efficient alternative to RuO_2.

ACKNOWLEDGMENTS

This work is funded by the Engineering and Physical Sciences Research Council under the EPSRC Supergen Energy Storage Consortium (Contract No. EP/D031672/1).

REFERENCES

1. H. Ibrahim, A. Ilinca, J. Perron. *Renew. Sustain. Energy Rev.* **12**, 1221 (2008).
2. E. Martinot, C. Dienst, L. Weiliang, C. Qimin. *Annu. Rev. Environ. Resour.* **32**, 205 (2007).
3. J. Larminie, A. Dicks. *Fuel Cells Systems Explained*, John Wiley, Chichester (2001).
4. B. E. Logan. *Microbial Fuel Cells*, John Wiley, New York (2007).
5. F. Zhao, N. Rahunen, J. Varcoe, A. Chandra, A. R. Claudio, A. Thumser, R. C. T. Slade. *Environ. Sci. Technol.* **42**, 4971 (2008).

6. S. R. Anton, H. A. Sodano. *Smart Mater. Struct.* **16**, R1 (2007).
7. A. Chandra, A. J. Roberts, R. C. T. Slade. *Solid-State Commun.* **147**, 83 (2008).
8. B. E. Conway. *Electrochemical Supercapacitors*, Kluwer Academia/Plenum, New York (1999).
9. V. L. Pushparaj, M. M. Shaijumon, A. Kumar, S. Murugesan, L. Ci, R. Vajtai, R. J. Linhardt, O. Nalamasu, P. M. Ajayan. *Proc. Natl. Acad. Sci. USA* **104**, 13574 (2007).
10. J. Chmiola, Y. Yushin, Y. Gogotsi, C. Portet, P. Simon, P. L. Taberna. *Science* **313**, 1760 (2006).
11. S. F. J. Flipsen. *J. Power Sources* **162**, 927 (2006).
12. J. N. M. Francoise, H. Gualous, R. Outbib, A. Berthon. *J. Power Sources* **143**, 275 (2005).
13. E. Karden, S. Ploumen, B. Fricke, T. Miller, K. Snyder. *J. Power Sources* **168**, 2 (2007).
14. R. Kotz, J.-C. Sauter, P. Ruch, P. Dietrich, F. N. Büchi, P. A. Magne, P. Varenne. *J. Power Sources* **174**, 264 (2007).
15. M. Mastragostino, F. Soavi. *J. Power Sources* **174**, 89 (2007).
16. P. Thounthong, S. Rael, B. Davat. *J. Power Sources* **158**, 806 (2006).
17. S. B. Ma, K. W. Nam, W. S. Yoon, X. Q. Yang, K. Y. Ahn, K. W. Oh, K. B. Kim. *Electrochem. Commun.* **9**, 2807 (2007).
18. V. Subramanian, H. Zhu, B. Wei. *J. Power Sources* **159**, 361 (2006).
19. C. Chen, D. Zhao, D. Xu, X. Wang. *Mater. Chem. Phys.* **95**, 84 (2006).
20. G. Wang, M. Qu, Z. Yu, R. Yuan. *Mater. Chem. Phys.* **105**, 169 (2007).
21. Y. G. Wang, Y. Y. Xia. *Electrochem. Commun.* **7**, 1138 (2005).
22. M. Wu, L. Zhang, D. Wang, C. Xiao, S. Zhang. *J. Power Sources* **175**, 669 (2008).
23. A. M. White, R. C. T. Slade. *Synth. Metal* **139**, 123 (2003).
24. F. Rouquerol, J. Rouquerol, K. Sing. *Adsorption by Powders and Porous Solids*, Academic Press, London (1999).
25. J. Rouquerol, D. Avnir, C. W. Fairbridge, D. H. Everett, J. H. Haynes, N. Pernicone, J. D. F. Ramsay, K. S. W. Sing, K. K. Unger. *Pure Appl. Chem.* **66**, 1739 (1994).